PERGAMON

International Journal of Heat and Mass Transfer 45 (2002) 1839–1847

International Journal of HEAT and MASS TRANSFER

www.elsevier.com/locate/ijhmt

Measurement of apparent solid-side mass diffusivity of a water vapor–silica gel system

Cheng-Chin Ni, Jung-Yang San *

Department of Mechanical Engineering, National Chung Hsing University, 250 Kuo-Kuang Road, Taichung, Taiwan, ROC

Received 26 April 2000; received in revised form 1 September 2001

Abstract

A measurement of the apparent solid-side mass diffusivity of water vapor adsorbed in a regular density silica gel is performed by using a constant-pressure thermal gravimetrical apparatus. The diameter of the silica gel particles is 2 mm. Six adsorption isotherms, individually correspond to 5.1, 22.2, 34.3, 49.5, 64.4 and 79.6 °C, are measured. The covered range of moisture content is from 0% to 40%. Using a previously developed model, which considers both surface (film) heat and mass transfer resistances, the measured uptake curves yield the apparent solid-side mass diffusivities. The apparent solid-side mass diffusivity is expressed as a function of temperature and moisture content. The thermal effect and importance of surface mass transfer resistance are individually discussed.

Keywords: Mass diffusivity; Silica gel; Adsorption; Moisture content; Isotherm

1. Introduction

Microporous solids are widely used in process of gas separation in industry. The performance of a microporous solid (adsorbent) in adsorption of a gas (adsorbate) is determined by its adsorption isotherms and solid-side mass diffusivity. The measurement of solid-side mass diffusivity is much more complicated than that of adsorption isotherms. Thus, up to the present, it is quite difficult to find a set of solid-side mass diffusivity data covering entire operating domain in the literature. For lack of this information, a theoretical Arrhenius-form solid-side mass diffusivity is oftenly used in simulation of the performance of adsorption systems [1–3]. Although in many cases it is quite successful using this theoretical solid-side mass diffusivity to yield an acceptable prediction. The measurement of solid-side mass diffusivity still remains as an interesting topic in research.

The solid-side mass diffusivity of an adsorption system can be determined by using several different approaches. Among them, traditional uptake rate measurement and modern nuclear magnetic resonance (NMR) measurement are the two most popular methods. The deviation of these two techniques was interpreted by Karger and Caro [4]. Many theoretical adsorption models were elaborated by Karger and Ruthven [5] and Ni and San [6]. The simplest approach for analyzing a constant-pressure microporous adsorption process is the isothermal model without external mass transfer resistance [7]. An adsorption system with thermal effect and convective heat transfer resistance was analyzed by Lee and Ruthven [8]. The apparent solid-side mass diffusivity of a rapidly diffusing system obtained from this model would be much greater than that obtained from the simple isothermal model. In many applications, adsorbate concentration boundary layer on the surface of adsorbent cannot be neglected and the external mass transfer (fluid film) resistance has to be considered. For such problems, the solution of a constant-pressure isothermal process with external mass transfer resistance is available [7]. As the Sherwood number approaches infinity, this solution would become the same as that of a simple isothermal model. The effect

* Corresponding author. Tel.: +886-011-4-22840432; fax: +886-011-4-22851941.

E-mail address: jysan@dragon.nchu.edu.tw (J.-Y. San).

0017-9310/02/$ - see front matter
PII: S0017-9310(01)00291-5

Nomenclature

a	external surface area per unit volume of adsorbent (m^{-1})
a_{1-6}	coefficients of κ
A_{1-2}	coefficients of isotherms
$b_{1-4,n}$	coefficients of D
B_{1-4}	coefficients of D
$B_{i,m}$	mass transfer Biot number, $h_m r_0/D$
c	gas concentration (kg m^{-3})
c_{1-6}	coefficients of ΔH
c_a	specific heat of adsorbent (kJ kg^{-1} K^{-1})
c_s^*	equilibrium gaseous phase concentration (kg m^{-3})
c_{sat}	saturated gas concentration (kg m^{-3})
D	apparent solid-side mass diffusivity (m^2 s^{-1})
D_0	constant (m^2 s^{-1})
h	convective heat transfer coefficient (W m^{-2} K^{-1})
h_{fg}	heat of vaporization (kJ kg^{-1})
h_m	convective mass transfer coefficient (m s^{-1})
ΔH	heat of sorption (kJ kg^{-1})
K	non-dimensional equilibrium constant, $\partial q^*/\partial c_s^*$
M_t	mass adsorbed at time t (kg)
M_∞	mass adsorbed at $t \to \infty$ (kg)
q	adsorbate concentration in solid (kg m^{-3})
q_m	average adsorbate concentration in solid (kg m^{-3})
q_n	characteristic roots
q_0	initial adsorbate concentration in solid (kg m^{-3})
q_∞	final adsorbate concentration in solid (kg m^{-3})
q^*	equilibrium adsorbed phase concentration (kg m^{-3})
Q	non-dimensional adsorbate concentration, $(q-q_0)/(q_\infty-q_0)$
Q_m	non-dimensional average adsorbate concentration, $(q_m-q_0)/(q_\infty-q_0)$
r	radial coordinate (m)
r_0	radius of particle (m)
R	gas constant (kJ kg^{-1} K^{-1})
t	time (s)
T	temperature (K or C°)
T_0	ambient gas temperature (K or C°)
w	moisture content

Greek symbols

α	time constant ratio, $har_0^2/(\rho_a c_a D)$
β	$\Delta H(\partial q^*/\partial T)/(\rho_a c_a)$
γ	$B_{i,m}/K$
η	non-dimensional coordinate, r/r_0
κ	bonding factor
θ	non-dimensional temperature, $-(\partial Q/\partial T)(T-T_0)$
ρ_a	wet adsorbent density (kg m^{-3})
τ	non-dimensional time, tD/r_0^2

of intraparticle heat conduction on a sorption process was investigated by Haul and Stremming [9] and Sun and Meunier [10]. The uptake curve of a constant-pressure sorption system with two coupled intraparticle mass diffusion resistances was obtained by Ruckenstein et al. [11].

The solution of a constant-volume sorption process is also available for isothermal systems [7]. As compared to the above constant-pressure sorption model, in evaluation of the solid-side mass diffusivity, the constant-volume sorption model has the advantage to reduce the size of corresponding apparatus. The thermal effect of a constant-volume sorption process was investigated by Kocirik et al. [12]. The uptake curve of a constant-volume sorption system with two coupled intraparticle mass diffusion resistances was obtained by Ma and Lee [13] and Lee [14].

The dynamic sorption of water vapor in silica gel was determined using a constant-volume apparatus by Lu et al. [15]. The experimental data yield the apparent solid-side mass diffusivity in the range 2×10^{-9}–2.5×10^{-11} m^2 s^{-1}. Andersson et al. [16] had investigated the dynamic sorption of water vapor in silica gel in a constant-pressure apparatus. It was found that the adsorption mechanism is solely controlled by heat transfer in the middle range of moisture content.

In this work, a constant-pressure thermal gravimetrical apparatus is designed to measure the apparent solid-side mass diffusivity of a water vapor–silica gel system. The measurement is conducted under atmospheric pressure. It is intended to obtain the data of apparent solid-side mass diffusivity and adsorption isotherms for industrial applications.

2. Mathematical model

A dynamic sorption model for a spherical microporous particle experienced with a small step change of gaseous phase adsorbate concentration was previously solved by Ni and San [5]. This solution is adopted in this work to match with the experimental data. The following assumptions are considered in the model: (i) micropore diffusion controls the mass diffusion in the solid, (ii) the temperature of the particle is uniform, (iii) both thermal effect and gas-side mass transfer resistance are

considered, (iv) the mass diffusivity is treated as a constant, (v) the concentration of gaseous phase adsorbate near the solid surface is in equilibrium with the adsorbed phase adsorbate on the solid surface. Based on the above assumptions, the non-dimensional mass conservation equation of the adsorbate can be expressed as follows:

$$\frac{1}{\eta^2}\frac{\partial}{\partial\eta}\left(\eta^2\frac{\partial Q}{\partial\eta}\right)=\frac{\partial Q}{\partial\tau} \tag{1}$$

with the initial and boundary conditions:

(i) at $\tau=0,\ Q=0$,
(ii) at $\eta=0,\ \partial Q/\partial\eta=0$,
(iii) at $\eta=1,\ (1/\gamma)(\partial Q/\partial\eta)=(1-Q)-\theta$.

The non-dimensional average concentration of adsorbate in the solid is

$$Q_m=3\int_0^1 Q\eta^2\,\mathrm{d}\eta. \tag{2}$$

The non-dimensional energy equation is

$$\beta\frac{\mathrm{d}Q_m}{\mathrm{d}\tau}=\frac{\mathrm{d}\theta}{\mathrm{d}\tau}+\alpha\theta \tag{3}$$

with the initial conditions: at $\tau=0,\ \theta=Q_m=0$.

The set of equations (1)–(3) were solved by using the Laplace transformation method. The solution is represented as follows [5]:

$$Q_m(\tau)=1-\sum_{n=1}^{\infty}\times\frac{\frac{3}{q_n^4}\exp(-q_n^2\tau)}{\frac{3\beta}{(q_n^2-\alpha)^2}+\frac{1}{2}\left[\left(-\frac{1}{\gamma}+\frac{3\beta}{q_n^2-\alpha}\right)^2+\frac{1}{q_n^2}\left(1-\frac{1}{\gamma}+\frac{3\beta}{q_n^2-\alpha}\right)\right]}, \tag{4}$$

$$\theta(\tau)=\sum_{n=1}^{\infty}\times\frac{-\frac{3\beta}{q_n^2(q_n^2-\alpha)}\exp(-q_n^2\tau)}{\frac{3\beta}{(q_n^2-\alpha)^2}+\frac{1}{2}\left[\left(-\frac{1}{\gamma}+\frac{3\beta}{q_n^2-\alpha}\right)^2+\frac{1}{q_n^2}\left(1-\frac{1}{\gamma}+\frac{3\beta}{q_n^2-\alpha}\right)\right]}, \tag{5}$$

$$Q(\eta,\tau)=1+\sum_{n=1}^{\infty}\times\frac{\frac{\sin(\eta q_n)}{\eta q_n^2\sin q_n}\left(-\frac{1}{\gamma}+\frac{3\beta}{q_n^2-\alpha}\right)\exp(-q_n^2\tau)}{\frac{3\beta}{(q_n^2-\alpha)^2}+\frac{1}{2}\left[\left(-\frac{1}{\gamma}+\frac{3\beta}{q_n^2-\alpha}\right)^2+\frac{1}{q_n^2}\left(1-\frac{1}{\gamma}+\frac{3\beta}{q_n^2-\alpha}\right)\right]}. \tag{6}$$

The values of q_n are determined by solving the roots of the following equation:

$$\frac{1}{q_n\cot q_n-1}=-\frac{1}{\gamma}+\frac{3\beta}{q_n^2-\alpha} \tag{7}$$

For $\gamma\to\infty$, the surface mass transfer resistance can be neglected. The uptake solution and corresponding characteristic equation can be deduced from Eqs. (4) and (7) as follows:

$$Q_m(\tau)=1-\sum_{n=1}^{\infty}\times\frac{\frac{3}{q_n^4}\exp(-q_n^2\tau)}{\frac{3\beta}{(q_n^2-\alpha)^2}+\frac{1}{2}\left[\left(\frac{3\beta}{q_n^2-\alpha}\right)^2+\frac{1}{q_n^2}\left(1+\frac{3\beta}{q_n^2-\alpha}\right)\right]}, \tag{8}$$

where

$$\frac{1}{q_n\cot q_n-1}=\frac{3\beta}{q_n^2-\alpha}$$

the above solution is the same as that derived by Lee and Ruthven [8].

For the case that the thermal effect is not important ($\alpha\to\infty$ or $\beta=0$), the uptake curve for isothermal adsorption with external film mass transfer resistance will be valid. This solution can be shown in the following form:

$$Q_m(\tau)=1-\sum_{n=1}^{\infty}\frac{6\gamma^2\exp(-q_n^2\tau)}{q_n^2\left[q_n^2+\gamma(\gamma-1)\right]}, \tag{9}$$

where

$$q_n\cot q_n+\gamma-1=0.$$

3. Experimental setup

A thermal gravimetrical apparatus (Fig. 1) is used to measure the uptake curves of a regular density silica gel in adsorption of water vapor. The silica gel particle has a diameter of 2 mm and density of 1270 kg m^{-3}. The mean pore diameter is 2 nm and its surface area is 508 m^2 g^{-1}.

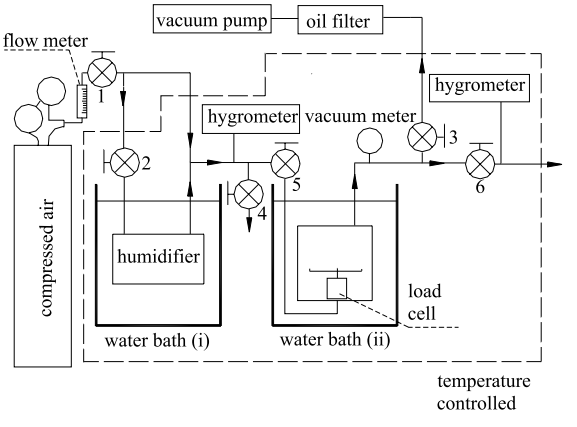

Fig. 1. Dynamic thermal gravimetrical apparatus.

Initially, 5.35 g of the silica gel particles (dry weight) are arranged in an oven for dehydration at 120 °C for 24 h. Then the dehydrated particles are placed on a 60-mesh stainless steel screen (10×10 cm^2) in a test chamber for another 3 h. The chamber is in a vacuum condition of 10^{-3} Torrs.

The spacing among the particles on the screen is important in this experiment. If the spacing is too small, the interaction among the particles will become important. Consequently, its sorption rate would be slower than that of a single particle in adsorption. This also can be known by observing the change of the color of dyed silica gel particles in a pan. The dyed silica gel particles initially are dehydrated in a heated oven. After exposing to ambient atmosphere for adsorption of water vapor, the color of the particles will change from blue to pink. A silica gel particle in a deep blue color stands for a very dry condition. Conversely, a light pink color stands for a wet condition. If the spacing among the particles is small, a longer time period is required for the particles to reach the same color as that of a single particle in adsorption. In this work, it is found that a minimum spacing of three times of particle diameter is necessary to elude the particle interaction effect.

The process air is supplied by the dehydrated air in a high pressure tank. After passing through two pressure regulators and valve 1 (Fig. 1), the air is divided into two streams. One is induced into a humidifier which is submerged in a water container. This humid air stream then is encountered with the other dry air stream for the use in the experiment. The humidity of the air can be directly controlled by regulating the air mass flowrate passing through valve 2. The water temperature in the container is controlled by a PID controller which insures a temperature variation within 0.2 °C. Two hygrometers (I-100, Rotronic) are individually installed in the inlet and outlet of the chamber to monitor the humidity change in the air stream.

The test chamber is made of stainless steel (Fig. 2). Its inner diameter is 155 mm and height is 240 mm. The air uniformly flows into the chamber from the bottom and it leaves from the top. In the chamber, the stainless steel screen is seated on a miniature load cell (LCFD-50, Omega). The signal of the load cell is picked up by using a data recorder (HR-1300, Yokogawa). The temperature difference between the inlet air and the wall of the chamber is minimized by using a temperature controlled water bath. Before entering the chamber the air is forced to flow through a 2 m long copper tube which is embedded in the same water bath as the test chamber. The temperature of the water bath either can be electrically heated for a high temperature adsorption or it can be controlled for a low temperature adsorption by passing cold water from a cooler through another copper coiler embedded in the same water bath.

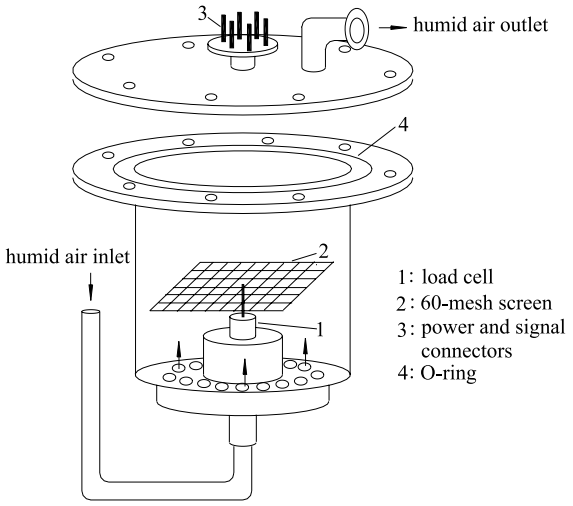

Fig. 2. Schematic of test chamber.

In the beginning of the measurement, dry silica gel particles are placed in the vacuum chamber which is embedded in water at a certain temperature. As the experiment starts, all the valves are open. The dry air mixed up with water vapor at a certain low humidity level flows into the chamber. At that moment, the silica gel particles proceed the adsorption of water vapor and the change of its weight is recorded for every time step. The air flowrate in the system is 10 l min^{-1}. This results in an average air velocity of 9.3×10^{-3} m s^{-1} in the test chamber. This velocity is low enough to assume that the air is quiescent. Consequently, the heat transfer data for free convection is suitable to be used later in the analysis. The required time period for the system to reach an equilibrium condition varies with temperature and moisture content. It decreases slightly with an increase of moisture content, however, it decreases significantly with an increase of temperature. The range of the time period varies between 1 and 16 h in the present work. As the system reaches an equilibrium condition, the valves at the inlet and outlet of the chamber are closed. After that, by regulating valve 2, the humidity ratio of the air flow can be controlled at another level for next measurement. For every temperature, eight or nine uptake curve measurements, which individually correspond to a different moisture content, are arranged. The weight of the particles at every equilibrium condition automatically constitutes the data of adsorption isotherm at that temperature.

There are several advantages for the measurement in the atmospheric condition over the measurement in a vacuum condition. First, the heat and mass transfer coefficients in the present system are easily obtained from free convection data and the analogy between heat and mass transfer. These data are also more reliable

than those usually used in a vacuum system. Second, the control of water vapor concentration is much easier in the present system than that in a vacuum system.

The main difference between the present measurement and that in a vacuum system is attributed to the effect of the air. It has been verified that the surface diffusion mechanism is the controlling factor for the adsorption of water vapor in regular density silica gels [1]. Thus the effect of the air on the apparent solid-side mass diffusivity is believed to be small. Neglecting the other factors which might affect the results of the two experiments, basically the two sets of data obtained by using the two different apparatus should reach a good agreement.

In this experiment, the maximum error on temperature measurement is 0.5% and that on water vapor concentration measurement is 2%. Based on these two values, an uncertainty analysis is performed [17]. For the isotherms, the maximum uncertainty is found to be less than 3%. For the solid-side mass diffusivity, the maximum uncertainty is 25%.

4. Adsorption isotherms

In this work, the adsorption isotherms are obtained by summarizing the final equilibrium data from each dynamic uptake rate measurement. Fig. 3 shows the adsorption isotherms of the system. Totally six adsorption isotherms are measured. The data of adsorption isotherms are curvefitted as a function of w and T as follows:

$$w(T,c) = (c\mathrm{e}^{-A_2})^{1/A_1}, \tag{10}$$

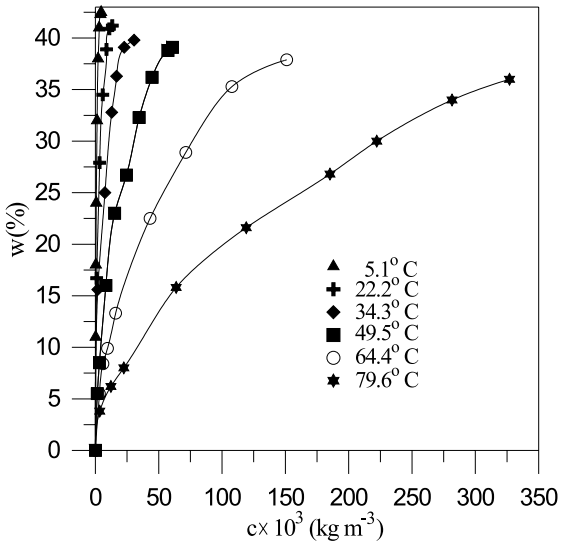

Fig. 3. Adsorption isotherms.

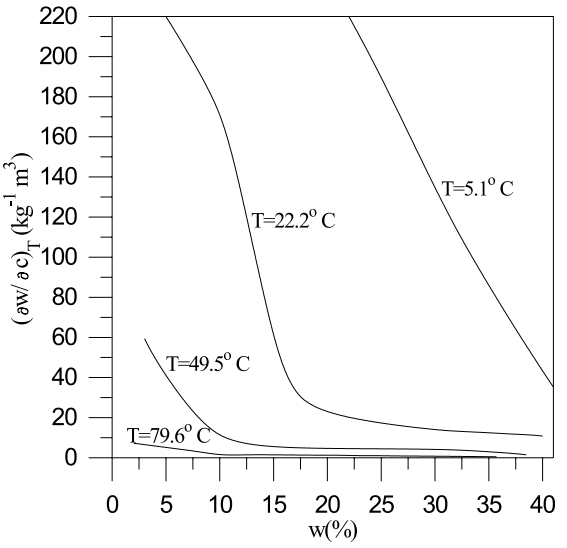

Fig. 4. $(\partial w/\partial c)_T$ of adsorption isotherms.

where for $0 \leqslant w \leqslant 0.4$ and $5\ ^\circ\mathrm{C} \leqslant T \leqslant 80\ ^\circ\mathrm{C}$

$$A_1 = -1.526(10)^{-6}T^3 + 5.075(10)^{-4}T^2 - 4.168(10)^{-2}T + 3.223$$

$$A_2 = 2.455(10)^{-4}T^2 + 3.721(10)^{-2}T + 3.793,$$

where T is in °C and c is in g m^{-3}. In the above equation, the mean deviation between the experimental data and curvefitting results is 9.3%. Figs. 4 and 5 individually indicate the variations of $(\partial w/\partial c)_T$ and $(\partial w/\partial T)_C$ for various values of w and T. These two derivatives are respectively used in evaluation of the β and γ in Eqs. (4)

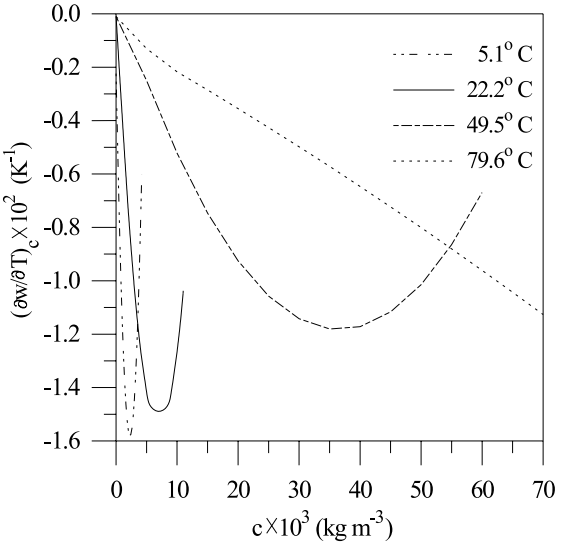

Fig. 5. $(\partial w/\partial T)_C$ of adsorption isotherms.

and (7). As shown in Fig. 4, the derivative, $(\partial w/\partial c)_T$, increases with decreasing of T. For the isotherm with a lower temperature, more adsorbate is adsorbed by the adsorbent. Thus the corresponding curve in Fig. 3 becomes steeper and the value of $(\partial w/\partial c)_T$ in Fig. 4 becomes larger. In Fig. 3, the slope of every individual isotherm decreases with an increase of c. Thus in Fig. 4, as the w increases, the corresponding $(\partial w/\partial c)_T$ decreases. Fig. 5 shows that, for every curve, there is a minimum $(\partial w/\partial T)_C$. This minimum point occurs almost at the c/c_{sat} of 0.5.

5. Results of uptake rate measurement

In Fig. 6, the theoretical uptake curves are evaluated by using two different non-isothermal models. One is with surface heat and mass transfer resistances and the other is only with surface heat transfer resistance (Lee and Ruthven's model [8]). As indicated, the matching of the former is much better than those of the latter. In Fig. 6, the apparent solid-side mass diffusivity obtained from the non-isothermal model with surface heat and mass transfer resistances is 2.1×10^{-9} m^2 s^{-1}, and that from Lee and Ruthven's model is 3.2×10^{-10} m^2 s^{-1}. This implies that the effect of surface mass transfer resistance on the apparent solid-side mass diffusivity is quite important. Without considering this factor, an underestimation of the value of D is possible.

Fig. 7 shows the matching of the experimental data with the theoretical results individually for w of 0.08 and 0.35. Two theoretical models are used. One is the non-isothermal model with surface heat and mass transfer resistances and the other is the isothermal model with surface mass transfer resistance. As shown in Fig. 7, for both the cases, the deviations between the experimental data and theoretical predictions are small. This implies that the thermal effect does not play an important role in these two processes. The thermal effect, in some cases, could be very important in predicting the uptake rate. However, in this case with the adsorption temperature of 22.2 °C, which is considered as a low temperature, the uptake rate is slow. Thus the generated heat will not accumulate in the particle to affect the process.

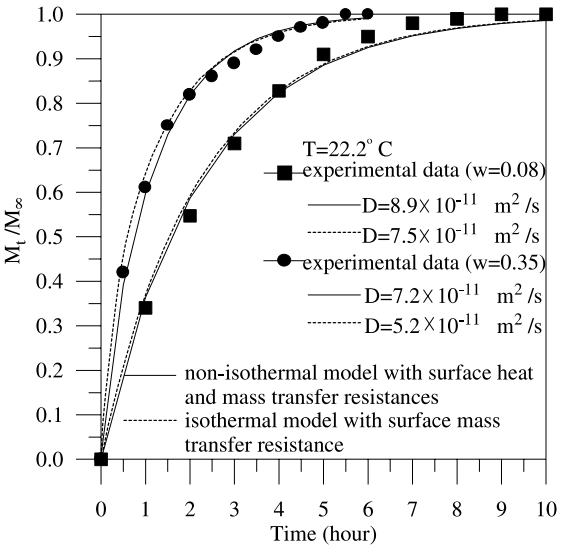

Fig. 7. Uptake curves for $T = 22.2$ °C.

Fig. 8 shows the uptake curves for w of 0.32 and T of 49.5 °C. The two lines individually possess the best

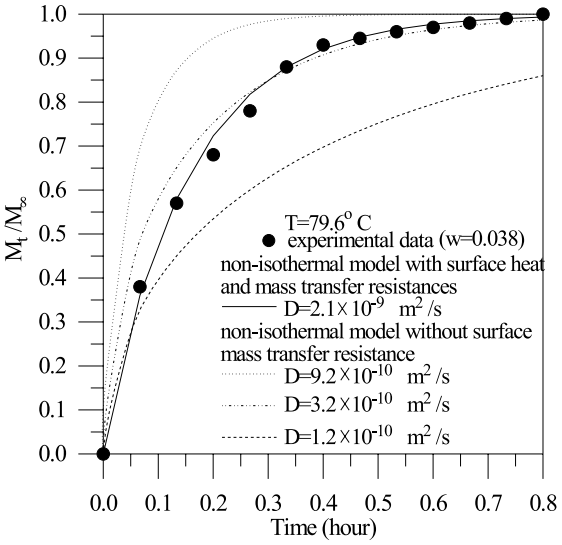

Fig. 6. Importance of surface mass transfer resistance.

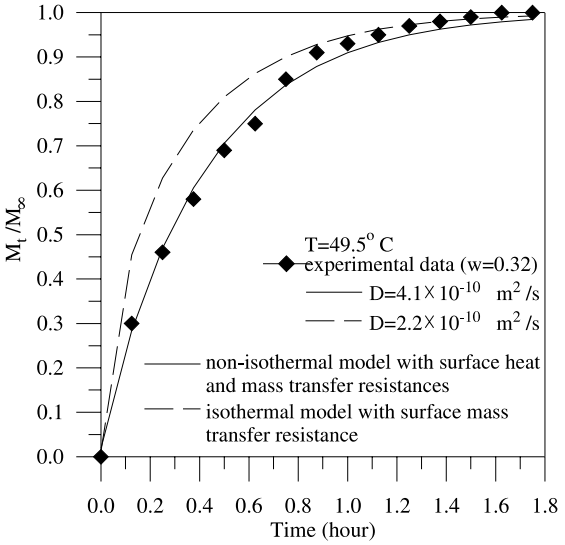

Fig. 8. Uptake curves for $T = 49.5$ °C.

matching of the experimental data with the corresponding theoretical uptake curves. The result reveals that the thermal effect is important in this case. Comparing the result obtained in Fig. 8 to that obtained in Fig. 7, it may find that the thermal effect is more important to the former than to the latter. If simply based on the information of the isotherms, for an adsorption process at a lower temperature, more water vapor is adsorbed and more heat is generated. Thus the thermal effect for a process at a lower temperature should be more important than that at a higher temperature. However, by observing the measured data in Figs. 7 and 8, it may find that the uptake rate at a higher temperature is much faster than that at a lower temperature. This makes the generated heat per unit time at a lower temperature actually is less than that at a higher temperature. In this work, the adsorption process proceeds in the atmospheric condition. The cooling due to air convection relieves part of the sorption heat generated in the silica gel particles. Thus the heat does not totally accumulate in the particles and the one with a higher generated heat per unit time would receive a greater impact from the thermal effect. However, if the experiment is performed in a vacuum condition, the cooling due to convection would be low. The generated heat would almost entirely accumulate in the particles to affect the uptake rate. Under this circumstance, the one adsorbs more water vapor would be the one receiving a greater impact from the thermal effect. In such case, the thermal effect would become more important for the process at a lower temperature.

The thermal effect and importance of external mass transfer resistance to an adsorption process also can be determined by evaluating the values of α/β and γ [2]. It had been shown that, for an increase of the value of α/β or for a decrease of the value of γ, the importance of the thermal effect will descend. In this work, for the equilibrium temperature of 5.1 °C, the value of γ is in the range 0.35–9.36 and α/β is in the range 26–105; for 22.2 °C, the value of γ is in the range 1.07–24.8 and α/β is in the range 21–132; for 49.5 °C, the value of γ is in the range 1.23–27.66 and α/β is in the range 5–26; for 79.6 °C, the value of γ is in the range 1.2–25.7 and α/β is in the range 2–16. Thus it implies that the higher the temperature, the greater the importance of the thermal effect. It also had been verified that, for the value of γ less than 100, the external mass transfer resistance cannot be ignored [5]. Applying this criterion to the present work, it may conclude that the external mass transfer resistance must be considered in all the above cases.

Many similar analyses as those in Figs. 6–8 are performed and the results are summarized in Figs. 9 and 10. In Fig. 9, the values of D correspond to the results obtained from the isothermal model with surface mass transfer resistance. In Fig. 10, the values of D correspond to the results obtained from the non-isothermal model with surface heat and mass resistances. Similar as those in Figs. 7 and 8, the higher the temperature, the greater the deviation between the results in Figs. 9 and 10. The comparison also indicates that, without considering the thermal effect, it may result in an underestimation of the apparent solid-side mass diffusivity. In Fig. 10, it shows that the apparent solid-side mass diffusivity increases with the temperature and its value falls in the range 2×10^{-9}–4×10^{-11} m^2 s^{-1}. For the case with the temperature less than 22.2 °C, the drop of the

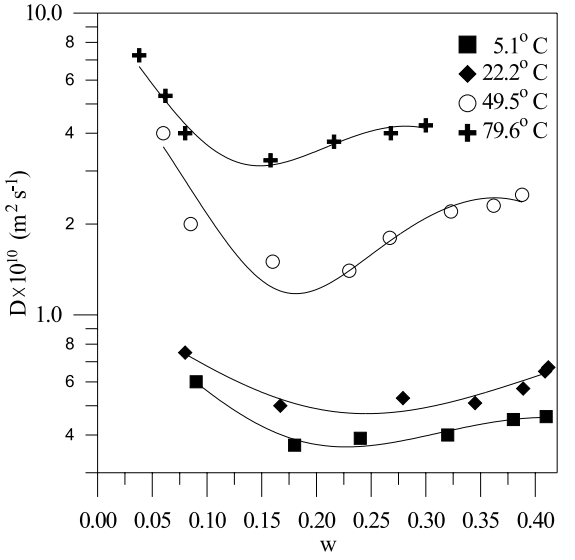

Fig. 9. Apparent solid-side mass diffusivity (isothermal model with surface mass transfer resistance).

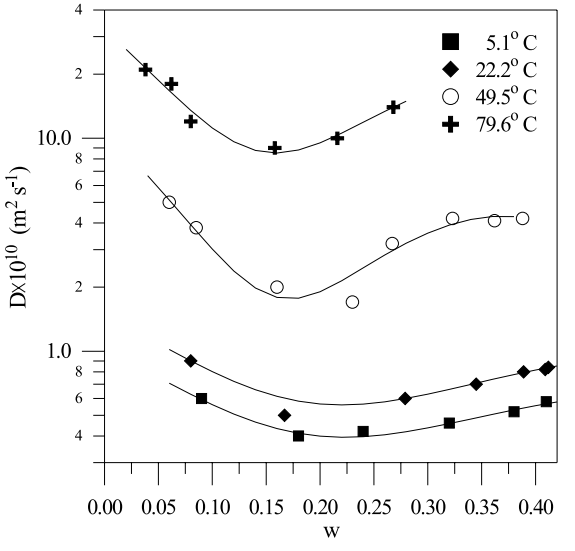

Fig. 10. Apparent solid-side mass diffusivity (non-isothermal model with surface heat and mass transfer resistances).

value of D seems sluggish for a further decrease of the temperature. This could be due to a low mobility of the adsorbed molecules on the adsorbent as the temperature approaches the freezing point of water at 0 °C.

In Fig. 10, for every curve there exists a minimum value of D for w near 0.2. For w less than 0.2, the adsorption occurs in the monolayer and the discrete hopping theory can be used to interpret the molecular migration in the pores [18]. Thus as the molecules in the adsorption sites increase, the hopping of the molecules will be sluggish and the apparent solid-side mass diffusivity descends. For w greater than 0.2, the adsorption no longer occurs in the monolayer and the self-diffusion mechanism for ordinary liquid dominates the migration of the molecules. In this situation, the D would increase with the w.

6. Regression analysis

In Fig. 10, the solid lines represent the curvefitting results. The corresponding polynomial and its coefficients are listed in Table 1, where T is in °C and w is in kg H_2O/kg silica gel. The mean deviation of this curvefitting is less than 6%. The set of data in Fig. 10 is also correlated into an Arrhenius-form equation with a mean deviation of 15% for $0.05 < w < 0.4$ and $5\ ^\circ\mathrm{C} \leqslant T \leqslant 80\ ^\circ\mathrm{C}$ as follows:

$$D = D_0 \exp\{\kappa[\Delta H/R(T + 273.15)]\}, \tag{11}$$

where

$$\kappa(w,T) = \frac{a_3 w^2 + a_2 w + a_1}{\{a_6(T + 273.15) + a_5 + [a_4/(T + 273.15)]\}h_{fg}},$$

$$a_1 = 2.638, \quad a_2 = 7.66, \quad a_3 = -12.77,$$

$$a_4 = 3.97, \quad a_5 = -2.41(10)^{-2}, \quad a_6 = 4.787(10)^{-5},$$

$$(-\Delta H/h_{fg}) = c_1 + c_2 w + c_3 w^2 + c_4 w^3 + c_5 w^4 + c_6 w^5,$$

$$c_1 = 1.911, \quad c_2 = -9.904, \quad c_3 = 62.708,$$

$$c_4 = -195.22, \quad c_5 = 291.47, \quad c_6 = -166.03,$$

$$h_{fg} = 2501.2 - 2.205T.$$

In Eq. (11), D_0 equals 1.6×10^{-6} m^2 s^{-1} and κ can be treated as the bonding factor between the adsorbent and adsorbate. ΔH is the heat of sorption (a negative value) which is evaluated by plotting the measured data of adsorption isotherms on an Othmer chart. Eq. (11) basically is in the same form as that used in Pesaran and Mill's work [1]. However, in the latter the bonding factor, κ, is a constant and in the former it is a function of w and T.

7. Conclusions

Both the dynamic uptake curves and equilibrium adsorption isotherms of the H_2O-silical gel system are successfully measured by using the constant-pressure thermal gravimetrical apparatus. The measured uptake data match well with the theoretical uptake curves. The apparent solid-side mass diffusivity deduced from the matching is correlated into an Arrhenius-form equation and its value is in the range 2×10^{-9}–4×10^{-11} m^2 s^{-1}.

The external mass transfer resistance is crucial in this experiment. Without considering this factor, the experimental data fail to match well with the theoretical uptake curves. Similarly, the thermal effect is also important to the adsorption uptake rate. Neglecting the thermal effect, it may result in an underestimation of the apparent solid-side mass diffusivity. Both the equilibrium temperature and moisture content determine the importance of the thermal effect in the adsorption processes. For an increase of the equilibrium temperature, the thermal effect will become more prominent regardless of the value of moisture content. However, as the equilibrium temperature is less than 22.2 °C, the thermal effect no longer seems to be important to the uptake rate. In this work, it is found that the apparent solid-side mass diffusivity decreases with the temperature. As the temperature approaching the freezing point of water (0 °C), the dependence of D on the temperature tends to be small.

For a specific equilibrium temperature, there exists a minimum apparent solid-side mass diffusivity in the considered range of water content. Before the occur-

Table 1
Coefficients of D

$D = \exp[f(w,T)] \times 10^{-10}$
$f(w,T) = B_1 + B_2 w + B_3 w^2 + B_4 w^3$
$B_n = b_{1,n} + b_{2,n} T + b_{3,n} T^2 + b_{4,n} T^3$

	B_1	B_2	B_3	B_4
$b_{1,n}$	1.7453	−18.7612	74.6515	−91.2916
$b_{2,n}$	−0.1773	2.9896	−13.1123	17.7364
$b_{3,n}$	7.6795×10^{-3}	−0.127663	0.54771	−0.7405
$b_{4,n}$	-7.4407×10^{-6}	4.7709×10^{-4}	-1.9091×10^{-3}	3.0279×10^{-3}

rence of the minimum point, the adsorption is in the monolayer and the discrete hopping theory for adsorbed molecules can be used to interpret the decrease of D for an increase of w. After the minimum point, it belongs to a multilayer adsorption and the theory of self-diffusion mechanism for ordinary liquid can be used to explain the increase of D for an increase of w.

References

[1] A.A. Pesaran, A.F. Mills, Moisture transport in silica gel packed beds – I, Int. J. Heat Mass Transfer 30 (1987) 1037–1049.

[2] J.Y. San, G.D. Jiang, Modeling and testing of a silica gel packed-bed system, Int. J. Heat Mass Transfer 37 (1994) 1173–1179.

[3] J.Y. San, Y.C. Hsu, Adsorption of toluene on activated carbon in a packed bed, Int. J. Heat Mass Transfer 41 (1998) 3229–3238.

[4] J. Karger, J. Caro, Interpretation and correlation of zeolitic diffusivities obtained from nuclear magnetic resonance and sorption experiments, J. Chem. Soc., Faraday Trans. I 73 (1977) 1363–1376.

[5] J. Karger, D.M. Ruthven, in: Diffusion in Zeolites and Other Microporous Solids, Wiley, New York, 1992, pp. 233–270.

[6] C.C. Ni, J.Y. San, Mass diffusion in a spherical microporous particle with thermal effect and gas-side mass transfer resistance, Int. J. Heat Mass Transfer 43 (2000) 2129–2139.

[7] J. Crank, in: Mathematics of Diffusion, Oxford University Press, Oxford, 1956, pp. 85–91.

[8] L.K. Lee, D.M. Ruthven, Analysis of thermal effects in adsorption rate measurement, J. Chem. Soc., Faraday Trans. I 75 (1979) 2406–2422.

[9] R. Haul, H. Stremming, Non-isothermal sorption kinetics in porous adsorbents, J. Colloid Interface Sci. 97 (1984) 348–355.

[10] L.M. Sun, F.A. Meunier, Detailed model for non-isothermal sorption in porous adsorbents, Chem. Eng. Sci. 42 (1987) 1585–1593.

[11] E. Ruckenstein, A.S. Vaidyanathan, G.R. Youngquist, Sorption by solids with bidisperse pore, Chem. Eng. Sci. 26 (1971) 1305–1318.

[12] M. Kocirik, P. Struve, M. Bulow, Analytical solution of simultaneous mass and heat transfer in zeolite crystals under constant-volume/variable-pressure conditions, J. Chem. Soc., Faraday Trans. I 80 (1984) 2167–2174.

[13] Y.H. Ma, T.Y. Lee, Transient diffusion in solids with a bipore distribution, AIChE J. 22 (1976) 147–152.

[14] L.K. Lee, The kinetics of sorption in a biporous adsorbent particle, AIChE J. 24 (1978) 531–534.

[15] L.T. Lu, D. Charoensupaya, Z. Lavan, Determination of sorption rate and apparent solid-side diffusivity of pure H_2O in silica gel using a constant volume/variable pressure apparatus, J. Solar Energy Eng. 113 (1991) 257–263.

[16] J.Y. Andersson, H. Bjurstrom, M. Azoulay, B. Carlsson, Experimental and theoretical investigation of the kinetics of the sorption of water vapor by silica gel, J. Chem. Soc., Faraday Trans. I 81 (1985) 2681–2692.

[17] S.J. Kline, F.A. McClintock, Describing uncertainties in single-sample experiments, Mech. Eng. 75 (1953) 3–8.

[18] E.R. Gilliland, R.F. Baddour, G.P. Perkinson, K.J. Sladek, Diffusion on surfaces. I. Effect of concentration on diffusivity of physically adsorbed gases, Ind. Eng. Chem. Fundam. 13 (1974) 95–99.